RSC Advances

RSC Advances

www.rsc.org/advances

ROYAL SOCIETY
OF CHEMISTRY

www.rsc.org/advances

1   **Design of a core-shell support to improve lipases features by immobilization**

2

3   Evelin A. Manoel [a,b,c,+], Martina Pinto [d,+], José C. S. dos Santos [c,e,+], Veymar G. Tacias-

4   Pascacio[b,f], Denise M. G. Freire [b], José Carlos Pinto *,[d] and Roberto Fernandez-Lafuente *,[b]

5   [a] Departamento de Biotecnologia Farmacêutica, Faculdade de Farmácia, Universidade Federal

6   do Rio de Janeiro, Rio de Janeiro, Brazil.

7   [b]Departamento de Bioquímica, Instituto de Química, Universidade Federal do Rio de Janeiro,

8   Rio de Janeiro, Brazil.

9   [c] Department of Biocatalysis, ICP-CSIC, Campus UAM-CSIC, Cantoblanco, 28049, Madrid,

10   Spain.

11   [d] Programa de Engenharia Química, COPPE, Universidade Federal do Rio de Janeiro, Rio de

12   Janeiro, Brazil.

13   [e]Instituto de Engenharias e Desenvolvimento Sustentável, Universidade da Integração

14   Internacional da Lusofonia Afro-Brasileira, CEP 62785-000, Acarape, CE, Brazil.

15   Unidad de Investigación y Desarrollo en Alimentos. Instituto Tecnológico de Veracruz, Calzada

16   Miguel A. de Quevedo 2779, 91897 Veracruz, Mexico

17   +: These coauthors have contributed equally to this paper.

18

19   * Co-corresponding authors:

20   José Carlos Pinto - Programa de Engenharia Química, COPPE/UFRJ/BRAZIL.

21   pinto@peq.coppe.ufrj.br

22   Roberto Fernandez-Lafuente - Department of Biocatalysis, ICP-CSIC / SPAIN.

23   rfl@icp.csic.es

24

25

Abstract: Two different core-shell polymeric supports, exhibiting different morphologies and composition, were produced through simultaneous suspension and emulsion polymerization, using styrene (S) and divinylbenzene (DVB) as co-monomers. Supports composed of polystyrene in both the core and the shell (PS/PS) and the new poly(styrene-co-divinylbenzene) support (PS-co-DVB/PS-co-DVB) were used for the immobilization of three different lipases (from *Rhizomucor miehie* (RML), from *Themomyces lanuginosus* (TLL) and the form B from *Candida antarctica*, (*CALB*)) and of the phospholipase Lecitase Ultra (LU). The features of the new biocatalysts were evaluated and compared to the properties of the commercial biocatalysts (Novozym 435 (CALB), Lipozyme RM IM and Lipozyme TL IM) and biocatalysts prepared by enzyme immobilization onto commercial octyl-agarose, a support reported as very suitable for lipase immobilization. It was shown that protein loading and stability of the biocatalysts prepared with the core-shell supports were higher than the ones obtained with commercial octyl-agarose or the commercial lipase preparations. Besides, it was shown that the biocatalysts prepared with the core-shell supports also presented higher activities than commercial biocatalysts when employing different substrates, encouraging the use of the produced core-shell supports for immobilization of lipases and the development of new applications.

Keywords: Polymeric supports; core-shell particles; lipase immobilization, hydrophobic supports, interfacial activation.

1.　　　Introduction

Enzyme immobilization enables the recovery and the reuse of these expensive biocatalysts as long as the preparation is stable enough [1–4]. Therefore, in order to benefit from this challenge, many efforts have been devoted to turn immobilization into the solution to other enzyme limitations, such as stability, activity, selectivity, specificity or purity [5–12].

Lipases are among the most used enzymes in biocatalysis, due to their characteristic wide specificity and the wide range of reactions that these enzymes can catalyze (including many promiscuous reactions) [13–15]. Besides, lipases show very high enantioselectivity [16–19] and are very robust, being successfully employed in different reaction media (e.g., aqueous media, organic solvents, neoteric media) [20,21].

The active centers of most lipases are secluded from the reaction media by a polypeptide chain (the lid), which is isolated from the medium by the large hydrophobic pocket where the active center is located (closed form) [24–27]. The lid can move and exposes this hydrophobic pocket to the medium, generating the open and active form of the lipase. This open lipase form readily adsorbs onto hydrophobic surfaces, including oil drops [22,28], hydrophobic supports [29], other open lipase molecules [30,31], other hydrophobic proteins [32].

In fact, a strategy that is becoming very popular for the immobilization of lipases is based on the interfacial activation of the enzyme on hydrophobic support surfaces [33]. This strategy allows the immobilization, purification and stabilization of the open lipase form (usually leading to hyper-activation), also producing an increase in the lipase stability for this reason [29]. It has been reported that the internal morphology or physical properties of the hydrophobic support may tune the lipase properties, including its activity, stability and specificity, [34–36]. Therefore, there is a great interest in the new development of new hydrophobic matrices that can further improve lipase properties. Among these new materials, core-shell polymeric particles, consisting of "large" particles (core) coated with small nano-particles (shell) may play a pivotal role [37–40].

3

75   Different techniques have been employed for the production of core-shell particles.

76   Among them, the combined suspension and emulsion polymerization process has special

77   interest. This technique typically comprises two fundamental steps. In the first step (suspension

78   polymerization), the particle cores are synthesized. When the monomer conversion reaches a

79   certain value in the core formation, the second step is initialized. To this goal, the elements of a

80   typical emulsion polymerization are fed into the reaction vessel. The new nanoparticles

81   coagulate over the previously prepared particle cores to form the shell. During the second

82   reaction step, the suspension and emulsion polymerization processes are conducted

83   simultaneously. At the end of the process, micrometric, porous and (in some cases)

84   functionalized polymer particles are obtained [40-41].

85   In the present manuscript, distinct polymeric supports presenting core-shell morphology

86   were produced through simultaneous suspension and emulsion polymerization, using styrene (S)

87   and divinylbenzene (DVB) as co-monomers. S and DVB are hydrophobic monomers, while

88   DVB can also promote chain crosslinking, leading to modification of the morphology and

89   mechanical resistance of the obtained polymer particles. The first step of this study comprised

90   the determination of how the co-monomers feed flow rate of S and DVB affects the specific area

91   and porosity of the synthesized core-shell particles. Afterwards, among the different supports

92   that were produced, one of them was selected for the enzyme immobilization procedure: the

93   support with the highest specific area (PS-co-DVB/PS-co-DVB). The previously described core-

94   shell polystyrene support (PS/PS), that has been successfully employed in the immobilization of

95   the lipase B from *Candida antarctica*, was also employed for comparison [41].

96   The prepared polymeric supports were used for the immobilization of three lipases:

97   lipases from *Rhizomucor miehei*, RML [42], from *Thermomyces lanuginosus*, TLL [43], and the

98   form B from *Candida antarctica*, CALB [44]. While CALB has a very small lid, which does not

99   completely isolate its active center from the reaction medium [45], TLL and RML exhibit very

100 large lids [46, 47]. The polymeric supports were also used for immobilization of the chimeric

4

101 artificial phospholipase Lecitase Ultra (LU) [48, 49]. PS/PS core-shell supports had been

102 previously and successfully used for CALB immobilization, but this is the first attempt to

103 immobilize the other enzymes on this support. The high specific area PS-co-DVB/PS-co-DVB

104 support is used to immobilize enzymes for the first time in this paper.

105   The new biocatalysts were compared with commercial biocatalysts (Novozym 435

106 (CALB), Lipozyme RM IM and Lipozyme TL IM) and biocatalysts prepared through enzyme

107 immobilization onto commercial octyl-agarose, a very popular support successfully used in

108 many instances for lipase immobilization[33,50]. Lipases immobilized on octyl-agarose have

109 been reported to be much more stable than the free enzyme, and even more than some lipases

110 immobilized via multipoint covalent attachment [51, 52]. This has been explained by the higher

111 stability of the adsorbed open form of the lipase compared to the lipase in conformational

112 equilibrium [53, 54]. Lipases tend to form dimeric aggregates with altered properties and that

113 may alter the results of the activity and stability studies and suggests that the use of free lipase to

114 compare the properties with immobilized enzymes may not be very adequate [55-59].

115

116

117

118   **2.   Materials and methods.**

119   **2.1. Materials.**

120   Solutions of CALB (19.11 mg of protein/mL), TLL (36 mg of protein/mL), RML

121   (13.7 mg of protein/mL) and of LU (16 mg of protein/mL), and the commercial immobilized

122   biocatalysts Novozym 435®, Lipozyme® TL IM and Lipozyme ® RM IM were kindly provided

123   by Novozymes (Spain). Octyl-Sepharose (octyl-agarose) beads were purchased from GE

124   Healthcare. Methyl mandelate, *p*-nitrophenyl butyrate (*p*-NPB) and triacetin were obtained from

125   Sigma Chemical Co. (USA).

126   Styrene supplied by Sigma Aldrich (USA) (minimum purity of 99.5% (wt/wt)) was

127   used as monomer for the production of PS/PS particles. For the production of PS-co-DVB/PS-

128   co-DVB particles, styrene was provided by INOVA (Brazil) and distilled under vacuum before

129   its use and DVB was supplied by Merck (USA).

130   Other reagents and solvents were of analytical grade and were used as received,

131   without any purification step.

132

133   **2.2. Preparation of core-shell polymeric supports and their characterization.**

134   Core-shell polymeric supports were synthesized through the combined suspension-

135   emulsion polymerization process [40, 41, 60-62]. The procedures used for production of

136   reference support PS/PS particles have been presented elsewhere [60]. However, modifications

137   of the original procedures were proposed here in order to increase the specific area and porosity

138   of the obtained polymeric particles.

139   Reactions were carried out in an open 1 L jacketed glass reactor (FGG Equipamentos

140   Científicos, São Paulo, Brazil) equipped with a thermostatic bath (Haake Phoenix II model,

141   Thermo Scientific, Karlsruhe, Germany) that was employed to keep the reactor temperature at

142   85°C. For the production of PS/PS particles, styrene was used as the only monomer in the

143   suspension and emulsion processes [60]. For the production of PS-co-DVB/PS-co-DVB,

6

144　copolymerization of styrene (75% (wt/wt) and DVB (25% wt/wt) was conducted during the

145　suspension and emulsion polymerization steps. For production of PS-co-DVB individual core

146　particles, classic suspension copolymerization was performed, without addition of the emulsion

147　feed.

148　　　　Initially, 100 g of an organic solution (containing the monomer mixture and 3.8%

149　(wt/wt) of the initiator benzoyl peroxide) were dispersed in 370 g of an aqueous solution

150　(containing distilled water and 0.80% (wt/wt) of poly(vinyl alcohol), used as stabilizer). The

151　dispersion was kept under continuous agitation (950 rpm in the PS/PS reaction and 800 rpm in

152　PS-co-DVB and PS-co-DVB/PS-co-DVB polymerizations) at a constant temperature of 85°C.

153　After two hours of reaction, the emulsion constituents (the monomer mixture and the aqueous

154　solution, containing distilled water, 0.13 wt% of the initiator potassium persulfate, 0.13%

155　(wt/wt) % of sodium bicarbonate and 1% (wt/wt) of sodium lauryl sulfate) were added to the

156　reaction medium. 30 g of the monomer mixture and 230 g of the aqueous solution were added as

157　a single load. The remaining 70 g of the monomer mixture were added under continuous flow

158　(0.026 L/h) in the PS/PS reaction [60]. For the production of PS-co-DVB/PS-co-DVB particles,

159　different flow rates were employed, as shown in Table 1. After feeding, two additional hours of

160　reaction were permitted to ensure the appropriate coverage of the core and formation of the

161　shell. Then, the reactor was cooled down to room temperature and the obtained particles were

162　filtrated and washed with cold water. Finally, the obtained polymer particles were dried in a

163　vacuum oven at 30°C until constant mass. The scheme of the polymerization process is shown in

164　Figure 1.

165　　　　The morphological characterization of the supports (specific area, average pore diameter

166　and volume of pores) was determined by nitrogen physisorption, using a surface analyzer

167　(ASAP 2020 model, supplied by Micromeritics, Norcross, GA, USA) and the obtained values

168　were adjusted using the BET model. Sample treatment was performed under vacuum at 60°C.

169　The average particle diameters were evaluated with a particle size distribution analyzer supplied

7

170   by Malvern Instruments (Master sizer Hydro 2000S model). Measurements were performed in

171   duplicates and the experimental errors were calculated with confidence level of 95%.

172   Polymer particles were also characterized by optical microscopy. The binocular

173   microscope (Nikon, model SMZ800 with capacity of $50 \times$ magnification) was equipped with a

174   digital camera (Nikon Coolpix 995), enabling the amplification and digitization of the images. A

175   Scanning Electron Microscope (Fei Company, Model Quanta 200) was also used to characterize

176   the obtained particles. Photomicrographs were processed in an image analyzer (Fei Company).

177   Typical morphological features of PS/PS particles have been described in previous publications

178   [60].

179

180   **2.2.1. Hydrolytic activity by *p*-NPB method and protein determination.**

181   The hydrolytic activities of the free or immobilized enzymes were determined by

182   measuring the increase of absorbance at 348 nm (isobestic point of *p*NP, ε is 5150 M^{-1}cm^{-1})

183   [63] produced by the release of *p*NP during the hydrolysis of 0.4 mM *p*-NPB in 50 mM sodium

184   phosphate at pH 7.0 and 25°C The reaction was initialized by adding 50–100 μL of the lipase

185   solution or suspension to 2.5 mL of the substrate solution. One international unit of activity (U)

186   was defined as the amount of enzyme that hydrolyzes 1 μmol of *p*-NPB per minute under the

187   previously described conditions. Protein concentration was determined following Bradford´s

188   method [64], using bovine serum albumin as the reference.

189

190   **2.2.2. Wetting of the different supports.**

191   PS/PS and PS-co-DVB/PS-co-DVB supports were pretreated to facilitate wetting. 1 g of

192   support was suspended in 10 mL of ethanol under slow stirring for 30 min, in order to fill the

193   support of solvent to remove air from the pores of the supports, facilitating the penetration of the

194   enzymatic solution. Afterwards, the support particles were filtrated, and suspended in 10 mL of

195   distilled water. The suspension was maintained under stirring for 30 min. Finally, the particles

196   were filtrated and washed with abundant distilled water.

197

198   **2.2.3. Immobilization of lipases on core-shell and octyl-agarose beads supports.**

199   CALB, TLL, RML and LU were immobilized onto the core-shell supports and octyl

200   agarose via interfacial activation. Standard immobilizations were performed using 1 mg of

201   protein per g of treated support to prevent diffusional constraints. To determine protein loading

202   capacity, the amount of enzyme was increased continuously until reduction of the

203   immobilization yield. In this case, enzyme immobilization was considered to be complete when

204   no significant changes of the supernatant activity could be detected after 4 h. Initially,

205   commercial enzyme solutions were diluted in 10 mM of sodium phosphate at pH 7 and $25°C$ to

206   give the desired enzyme concentrations. Then, the supports were added to the diluted enzyme

207   solutions. The activities of both supernatant and suspension were measured using *p*-NPB. At the

208   end of the immobilization process, suspensions were filtrated and the immobilized enzymes

209   were washed several times with distilled water.

210

211   **2.2.4. Study of the stability of the different biocatalysts.**

212   **2.2.4.1. Thermal inactivation of different immobilized enzymes.**

213   1 g of immobilized enzyme was suspended in 10 mL of 25 mM of sodium phosphate

214   at pH 7 at different temperatures to force enzyme inactivation (reaction conditions were selected

215   in order to obtain inactivation rates based on reliable data in a reasonable time). Then, samples

216   were withdrawn and the enzymatic activity was measured using the *p*-NPB method described

217   above. The half-lives were calculated from the observed inactivation courses.

218   **2.2.4.2. Inactivation of different immobilized enzymes in the presence of organic co-**

219 **solvents**

220   Biocatalysts were incubated in mixtures of 90% (V/V) DMF (dimethylformamide) and

221 10% (V/V) of 100 mM Tris–HCl. The pH of the inactivating solution was adjusted at 7 before

222 adding the immobilized enzymes at 4°C. Then, the temperature was set to 25°C. Then, samples

223 were periodically withdrawn and the enzymatic activity was measured with the *p*-NPB assay.

224 The half-lives were calculated from the observed inactivation courses. The addition of 90 μL of

225 DMF during the activity tests did not affect the observed activity.

226

227 **2.2.5. Hydrolysis of methyl mandelate.**

228   Enzymatic activity was also evaluated using methyl mandelate as substrate and the

229 respective maximum loaded biocatalysts. 1 g of immobilized enzyme was added to 10 mL of 50

230 mM methyl mandelate dissolved in 50 mM sodium phosphate at pH 7 and 25°C under

231 continuous stirring. Substrate conversions were determined using a RP-HPLC (Spectra Physic

232 SP 100) coupled with an UV detector (Spectra Physic SP 8450) and a Kromasil C18 (15 cm ×

233 0.46 cm) column (Análisis vinicos, Spain). During analysis, 20 μL of each sample were injected

234 in the column at a flow rate of 1.0 mL/min utilizing a solution of acetonitrile: 10 mM

235 ammonium acetate (35:65, v:v) (pH=2.8) as mobile phase and the absorbance at 230 nm was

236 recorded (retention times were 2.4 min for mandelic acid   and 4.2 min for methyl mandelate).

237 One unit of enzyme activity was defined as the amount of enzyme necessary to produce 1 μmol

238 of mandelic acid per minute under the conditions described above. Each reaction was executed

239 in triplicate with a maximum conversion of 15–20 %. Reported data are based on average

240 values.

241

242 **2.2.6. Hydrolysis of triacetin.**

243 Maximum loaded biocatalysts were also used in the hydrolysis of triacetin. Solutions

244 of 100 mM triacetin in 100 mM sodium phosphate at pH 7 were prepared. 1 g of the biocatalyst

245 was added to 50 mL of the substrate solution. Reactions were performed under stirring at 25°C.

246 Samples were periodically withdrawn from reaction suspensions. The biocatalyst was discarded

247 by centrifugation and the concentration of products in the supernatant was analyzed by HPLC. A

248 solution of 10% acetonitrile/water (v/v) was used as the mobile phase and a Kromasil C18

249 column (15cm×0.46 cm) was employed. A RP-HPLC (Spectra Physic SP 100) coupled with an

250 UV detector Spectra Physic SP 8450 (detection was performed at 230 nm) were used (retention

251 times of 32.0 min for triacetin, 5.8 min for 1,2-diacetin and 4.8 min for 1,3-diacetin) [65].

252 Concentrations of triacetin were calculated based on calibration curves using real samples.

253 Reactions were performed in triplicates with maximum conversions of 15–20% and the reported

254 data are based on the mean of the obtained values.

255

256 **3.   Results and Discussion.**

257 **3.1.   Influence of the polymerization conditions on the morphology of the supports.**

258   Figure 2 shows that the increase in the co-monomer feed flow rate causes a decrease in

259 the average particle diameter. Probably higher co-monomer feed flow rates destabilize the

260 emulsion media, increasing the agglomeration of the emulsified nanoparticles thus diminishing

261 the average core-shell particle diameter. However, the average particle diameters are still on the

262 micrometric scale even using high flow rates.

263   Figure 3 illustrates the influence of the co-monomer feed flow rate on the morphology of

264 the polymeric particles. Considering the specific area (Figure 3A) and the volume of pores

265 (Figure 3B) of the core-shell particles, there was a particular range on the monomer feed flow

266 rate that resulted in particles with pronounced specific area and porosity. However, apparently

267 the comonomer feed flow rate did not affect the average pore diameter of the particles (Figure

268 3C). Probably, a low co-monomer feed flow rate (0.019 L/h) provided a longer time for the

269 coating of the cores (that could result in higher specific area and more porous particles).

270 However, it may also cause greater stability of the emulsified particles, and that may result in

271 lower core coatings and lower specific area of the core-shell particles. Moreover, a high co-

272 monomer feed flow rate caused a destabilization of the emulsion, resulting in larger

273 agglomeration of particles (both the core and the shell nanoparticles) and in a decrease of the

274 specific area and the porosity. Therefore, regarding the enzyme immobilization procedure, only

275 one support among the ones that were obtained was evaluated: the one having the highest

276 specific area support (produced on reaction 7), called PS-co-DVB/PS-co-DVB. The support

277 PS/PS was used for comparison.

278

279 **3.2. Morphological aspects of the synthesized supports employed on enzyme**

280   **immobilization.**

281   The morphological aspect of PS-co-DVB/PS-co-DVB and PS/PS core-shell particles and

282   also the PS-co-DVB core particles are illustrated in Figure 4. The compact PS-co-DVB core

283   particles were much smaller than the core-shell particles and exhibited a well-defined spherical

284   morphology. The PS/PS core-shell particles were larger and presented characteristic irregular

285   surfaces. Comparing both types of core-shell particles, it can be noted that the new PS-co-

286   DVB/PS-co-DVB particles showed much more regular spherical appearance and were smaller

287   than PS/PS particles. Figure 5 shows that core-shell particles become more irregular and much

288   larger when the emulsified particles agglomerate over the cores to form the shell structure.

289   Formation of the porous shell is clearly visualized in Figure 5C.

290   Considering the wide range of likely applications for the produced supports, the average

291   particles diameter is important since it may condition their handling. Very small particles would

292   require the use of complex methods for separation of biocatalysts from the reaction media at the

293   end. Very large particles can intensify diffusional problems. Therefore, the production of

294   micrometric support particles is desirable and can facilitate the industrial use of the biocatalysts.

295   The average particle diameters of the supports that will be used on the enzyme immobilization

296   process are shown in Table 2. The produced supports presented average particle diameters of

297   approximately 100 μm. PS/PS particles were the largest ones. It can also be noticed that the

298   average diameters of the new PS-co-DVB/PS-co-DVB core-shell particles were smaller than

299   those of the corresponding core particles. This was due to coagulation of nanoparticles during

300   the emulsion step, which shifted the average particle sizes towards smaller values. Nevertheless,

301   the particles were still on the micrometric scale, which is advantageous for separation processes.

302   Table 3 shows the specific area, the average pore diameter and the volume of pores of

303   the produced core-shell particles. These results clearly indicate the formation of the shell over

304   the particle cores, as the core presents negligible specific area when compared to the core-shell

305   supports.

306   Comparing the core-shell supports, the specific area and porosity were higher for the

307 new PS-co-DVB/PS-co-DVB particles, indicating that the small modifications of the

308 implemented operation procedures utilized in the preparation of these new materials allowed the

309 production of more porous matrices. The presence of DVB to the reaction media leads to an

310 increase in the particle porosity because DVB promotes chain crosslinking, changing the

311 microstructure of polymeric particles, as discussed in previous works [41]. Besides, the increase

312 of the feed flow rate during the emulsion step (0.069 L/h instead of 0.04 L/h, as in the previous

313 study [41]) allowed the production of higher amounts of nanoparticles in shorter reaction times,

314 increasing the desired core coverage without increasing the rate of undesired agglomeration of

315 the support particles.

316   It is possible to observe in Table 3 that the average pore sizes of the supports ranged

317 from 200 Å (PS-co-DVB/PS-co-DVB) to 290 Å (PS/PS), which are wide enough to permit the

318 diffusion of even moderately large protein molecules. As the core compact particles exhibited

319 negligible specific areas, they were not used for enzyme immobilization studies; they were used

320 only to evaluate the shell coverage on the core-shell particles synthesis.

321   According to Cunha *et al.* (2014) [41 all of these different supports should exhibit

322 similar hydrophobicities. This indicates that distinct interactions between the polymeric supports

323 and the enzymes should be mainly caused by differences of the surface characteristics of the

324 particles (area, internal morphology). Moreover, as the synthesized supports are hydrophobic,

325 lipases should tend to become interfacially activated versus their surface, and this should be the

326 main cause for the immobilization procedure [29].

327

328　**3.3.**　　**Performance of the different supports on the immobilization of the different**

329　　　　**enzymes.**

330　　**3.3.1.　Effects on the activity.**

331　　Figure 6 shows the immobilization courses using low enzyme loading (10-20 pNPB U)　to

332　prevent diffusional problems that could alter the results. Immobilization using these low

333　loadings is almost total and very rapid for all assayed supports and enzymes. Moreover, all three

334　supports allowed the increase of the enzymes activity upon immobilization, ranging from 109%

335　(octyl-agarose-CALB) to 377% (octyl-agarose-RML). This increase in enzyme activity has been

336　previously reported and derived from the stabilization of the open form of the lipases [33]. In

337　most cases, the new PS-co-DVB/PS-co-DVB was the support that gave the highest activity

338　(except for RML, in this case octyl-agarose gave the lowest activity), and PS/PS gave the lowest

339　activities (except for CALB, the enzyme where octyl-agarose gave the lowest activity).

340

341　**3.3.2.　Determination of the loading capacity of the different core-shell supports.**

342　　　The immobilization yields at different protein concentrations of CALB, RML, LU and

343　TLL on the different supports are illustrated in Figures S1, S2 and S3 (supporting information).

344　The new PS-co-DVB/PS-co-DVB particles immobilized the activity contained in 65 mg/g of

345　CALB, 120 mg/g of RML, 55 mg/g of LU and 65 mg/g of TLL (Figure S1 (A-D)). When PS/PS

346　supports were employed, the maximum enzymatic loadings were lower regardless the analyzed

347　enzyme (around 55-70% of the results obtained using PS-co-DVB/PS-co-DVB sore-shell

348　particles, depending on the lipase) (Fig. 2S (A-D)). This result reflected the lower specific areas

349　of PS/PS (around 80% of the specific area of PS-co-DVB/PS-co-DVB particles), and the

350　success in the new design of the core-shell process. The differences between loading capacity

351　and specific area may be due to changes of both supports under wet conditions, as apparently

352　PS/PS supports took 20% more water than PS-co-DVB/PS-co-DVB, which can explain the

353　differences because we used wet supports weights in the immobilization experiments.

15

354 Moreover, the dynamics of the polymer chains can be very different in both supports, as the

355 copolymer chains crosslinked by DVB became more rigid and this may somehow affect the

356 final support performance. Octyl-agarose was able to immobilize around 20 mg/g of CALB, 15

357 mg/g of RML 22 mg/g of TLL and 27 mg/g using LU (Figure 3S). Thus, both core-shell

358 supports showed higher enzyme loading capacities than octyl agarose, which is considered a

359 very good support for lipase immobilization [50].

360

361 ### 3.3.3. Stability of the different biocatalysts under different conditions

362 Table 4 shows the half-lives of the different immobilized enzymes when subjected to

363 thermal inactivation conditions at pH 7 and in the presence of DMF. It is important to point out

364 that the most stable biocatalysts depended on the enzyme nature and on the inactivation

365 conditions; there was not a "universal" optimal support for the four enzymes. PS-co-DVB/PS-

366 co-DVB-CALB was more stable in thermal inactivation than PS/PS-CALB but it was less stable

367 in presence of DMF. The results using TLL and LU biocatalysts showed the opposite behavior.

368 On the other hand, PS-co-DVB/PS-co-DVB-RML biocatalyst was always more stable than the

369 other core-shell preparation. Octyl-agarose-CALB (a support that has been reported that may

370 stabilize lipases hundreds folds compared to the free lipase) [66] exhibited a thermal stability

371 that was similar to the thermal stability of PS-co-DVB/PS-co-DVB-CALB, but it was

372 significantly less stable in DMF medium. Octyl-agarose-TLL was the most stable TLL

373 biocatalyst under thermal inactivation conditions, but was less stable than PS-co-DVB/PS-co-

374 DVB-TLL under solvent inactivation conditions. Finally, PS-co-DVB/ PS-co-DVB-LU

375 presented the lowest thermal stability but it was the most stable under solvent inactivation

376 conditions. . The lipase preparations were also inactivated at pH 5 and 9, the differences in the

377 stabilities between the different biocatalysts were maintained (see Table 1S).

378 Therefore, the relative stability of the preparations depends on the enzyme and also on

379 the inactivating agent, although, in general, in the presence of organic co-solvents the better

380   performance of the new core-shell biocatalysts seems clear. Perhaps the high hydrophobicity of

381   the produced particles permits a stronger enzyme adsorption on the support, when compared to

382   octyl-agarose biocatalysts. This may reduce the release of the enzyme to the medium in the

383   presence of organic solvents, being the main reason for lipase inactivation in organic solvent

384   during incubation in high organic cosolvent concentration solutions [6].

385

386   **3.3.4. Enzyme activity *versus* different ester substrates.**

387   All biocatalysts were evaluated in hydrolysis reactions of two compounds with very

388   different structures, triacetin and methyl mandelate (the R and the S isomers) (Tables 5 and 6,

389   respectively). These assays were performed in order to check if the specificity of the enzyme

390   may be altered after immobilization on supports having different properties even if the

391   mechanism of immobilization is similar, as observed in other works [6].

392   Using CALB biocatalysts in the hydrolysis of triacetin, the least active biocatalyst was

393   octyl-agarose-CALB followed by PS-co-DVB/PS-co-DVB-CALB. PS/PS-CALB was slightly

394   more active than the commercial and widely used Novozym 435 with this substrate (Table 5).

395   However, in the hydrolysis of R methyl mandelate, Novozym 435 had the lowest activity while

396   the new PS-co-DVB/PS-co-DVB-CALB was the most active, with octyl-agarose-CALB and

397   PS/PS-CALB exhibiting similar activities (Table 6). All preparations preferred the R isomer

398   with a moderate enantiopreference, although PS-co-DVB/PS-co-DVB-CALB doubled the ratio

399   VR/VS compared to Novozym 435.

400   Analyzing RML biocatalysts, the most active one using both substrates was the new PS-

401   co-DVB/PS-co-DVB-RML (Tables 5 and 6). The second most active biocatalyst depended on

402   the employed substrate: it was PS/PS-RML using triacetin, while using methyl mandelate as

403   substrate, the second most active was octyl-agarose-RML. The commercial preparation was the

404   catalyst with the lowest activity in both cases. In this case, the preferred isomer was the S, with

405   activity ratios between both isomers ranging from 3 to 4 (Table 6).

17

406   Considering TLL immobilized preparations, the most active biocatalysts in triacetin

407   hydrolysis were both core-shell supports, shortly followed by octyl-agarose-TLL and both of

408   them doubling the activity of the commercial preparation (Table 5). Using R methyl mandelate,

409   PS-co-DVB/PS-co-DVB-TLL was the most active; octyl-agarose-TLL and PS/PS-TLL showed

410   around half of that activity, shortly followed by the commercial preparation (Table 6). The

411   preference for the R isomer was scarce (ranging from 1.57 using octyl-agarose-TLL to 2.3

412   employing the commercial preparation).

413   LU biocatalysts exhibited short differences using triacetin as substrate, being PS-co-

414   DVB/PS-co-DVB-LU the most and PS/PS the least active one (Table 5). However, PS-co-

415   DVB/PS-co-DVB-LU was 2.5 fold more active than the other two biocatalysts using R methyl

416   mandate as substrate, (Table 6). The enantiopreference was very low, but while PS-co-DVB/PS-

417   co-DVB-LU preferred the R isomer, the other two preparations preferred the S isomer (Table 6).

418   It was possible to observe generally better hydrolytic activities of the new biocatalysts,

419   mainly the enzymes immobilized in the new PS-co-DVB/PS-co-DVB core-shell support,

420   compared to the commercial ones. More interestingly, it was noticed that even though the

421   immobilization of all home-made biocatalysts involved interfacial activation as immobilization

422   mechanism, the final properties of each one were strongly modulated by the exact nature of the

423   support. Thus, the most active biocatalyst produced using a specific support may exhibit a low

424   hydrolytic activity when other substrate were investigated, as reported in many other cases [6].

425   Another important feature of an immobilized enzyme is its operational stability. To this

426   goal, each enzyme biocatalyst was employed on 5 consecutive cycles of hydrolysis of triacetin .

427   After each cycle, the biocatalysts were washed 3 times with 3 volumes of 20 mM sodium

428   phosphate. All the biocatalysts, including the commercial biocatalysts, those prepared using

429   octyl-agarose and core-shell biocatalysts, showed a decrease of activity under 20% along the 5

430   reaction cycles, as shown in Figure 7.

431

432　**4.　Conclusion**

433　　　　　The new hydrophobic core-shell support (PS-co-DVB/PS-co-DVB) developed in the

434　present work showed high protein loading capacity, exceeding the capacity of commercial octyl-

435　agarose supports, known for its very good performance [33] and that of the previously described

436　PS/PS core shell [41]. This high enzyme loading capacity is obtained by the porous shell of the

437　produced polymeric core/shell particles, as we have shown that the core loading capacity is

438　negligible. However, the core particles are critical to produce stable particles [61].

439　　　　　The new biocatalysts were much more stable than the commercial biocatalysts or the

440　ones obtained using octyl-agarose in many instances but not always. This higher stability was

441　mainly observed in organic solvents inactivations, where enzyme desorption play an important

442　role in the biocatalyst stability and the more hydrophobic nature of the new PS-co-DVB/PS-co-

443　DVB should reduce the enzyme release [67]. However, considering each enzyme and each

444　inactivation condition, it seems that there is not an absolute "optimal" immobilization support

445　from those here studied regarding enzyme stability.

446　　　　　Finally, the activities of the new biocatalysts employing distinct substrates were much

447　higher than the ones obtained with commercial products, except when triacetin was hydrolyzed

448　by CALB . Moreover, in many cases, the enzymatic activities were also much higher than the

449　ones observed when octyl-agarose was used as support. As it has been previously reported [35],

450　the chemical and textural properties of the support surfaces alter the final lipase performance

451　even if the immobilization mechanism is in all cases interfacial activation. Thus, the use of

452　differently prepared hydrophobic core shell supports may be a way to enrich a library of lipase

453　biocatalysts [68].

454　　　　　Based on the obtained results, it can be concluded that changing some operational

455　conditions during the polymerization reaction, such as the co-monomer feed flow rate, it is

456　possible to synthesize core-shell particles with distinct morphological aspects. Moreover, among

457   the different core-shell supports that were produced, the new PS-co-DVB/PS-co-DVB

458   constitutes a very promising support for lipase immobilization.

459

467

468

469   **References**

470   [1]   Chibata I., Tosa T., Sato T., J. Mol. Catal., 1986, **37,** 1–24.

471   [2]   Hartmeier W., Trends Biotechnol., 1985, **3**, 149–153.

472   [3]   Katchalski-Katzir E., Trends Biotechnol., 1993, **11**, 471–478.

473   [4]   Kennedy J.F., Melo E.H.M., Jumel K., Chem. Eng. Prog., 1990, **86**, 81–89.

474   [5]   Fernandez-Lafuente R., Enzyme Microb. Technol., 2009, **45**, 405–418.

475   [6]   Mateo C., Palomo J.M., Fernandez-Lorente G., Guisan J,M., Fernandez-Lafuente R.,

476   Enzyme Microb. Technol., 2007, **40**, 1451–1463.

477   [7]   Petkar M., Lali A., Caimi P., Daminati M., J. Mol. Catal. B Enzym., 2006, **39**, 83–90.

478   [8]   Rodrigues R.C., Ortiz C., Berenguer-Murcia Á., Torres R., Fernández-Lafuente R.,

479   Chem. Soc. Rev., 2013, **42**, 6290–6307.

480   [9]   Hernandez K., Fernandez-Lafuente R., Enzyme Microb. Technol., 2011, **48**,107–22.

481   [10]   Guzik U., Hupert-Kocurek K., Wojcieszyńska D., Molecules, 2014,**19**, 8995–9018.

482   [11]   Garcia-Galan C., Berenguer-Murcia Á., Fernandez-Lafuente R., Rodrigues R.C., Adv.

483   Synth. Catal., 2011, **353**, 2885–2904.

484   [12]   Barbosa O., Ortiz C., Berenguer-Murcia A., Torres R., Rodrigues R.C., Fernandez-

485   Lafuente, R., Biotechnol. Adv., 2015, **33**, 435-456.

486   [13]   Carboni-Oerlemans C., Domínguez de María P., Tuin B., Bargeman G., Van der Meer A.,

487   Van Gemert R. J., Biotechnol., 2006, **126**, 140–151.

488   [14]   Humble M.S., Berglund P., European J. Org. Chem., 2011, 3391–3401.

489   [15]   Kapoor M., Gupta M.N., Process Biochem., 2012, **47**, 555–569.

490   [16]   Jaeger K.E., Eggert T., Curr. Opin. Biotechnol., 2002, **13**, 390–397.

491   [17]   Adlercreutz P., Chem. Soc. Rev., 2013, **42**, 6406–6436.

492   [18]   Sharma R., Chisti Y., Banerjee U.C., Biotechnol. Adv., 2001, **19**, 627–662.

493   [19]   Jaeger K.E., Reetz M.T., Trends Biotechnol., 1998, **16**, 396–403.

494   [20]   Lozano P., Green Chem., 2010, **12**, 555-569.

495   [21]   Lozano P., Garcia-Verdugo E., Luis S., Pucheault M., Vaultier M., Curr. Org. Synth.,

496   2011, **8**, 810–823.

497   [22]   Verger R., Trends Biotechnol., 1997, **15**, 32–38.

498   [23]   Cambillau C., Longhi S., Nicolas A., Martinez C., Curr. Opin. Struct. Biol., 1996, **6**, 449–

499   455.

500   [24]   Brzozowski A.M., Derewenda U., Derewenda Z.S., Dodson G.G., Lawson D,M.,

501   Turkenburg J.P. *et al.*, Nature, 1991, **351**, 491–494.

502   [25]   Kim K.K., Song H.K., Shin D.H., Hwang K.Y., Suh S.W., Structure 1997, **5**, 173–185.

503   [26]   Jaeger K.E., Ransac S., Koch H.B., Ferrato F., Dijkstra B.W., FEBS Lett., 1993,

504   **332**,143–149.

505   [27]   Cygler M., Schrag J.D., Biochim. Biophys. Acta, 1999, **1441**, 205–214.

506   [28]   Reis P., Holmberg K., Watzke H., Leser M.E., Miller R., Adv. Colloid Interface Sci.,

507   2009, **147-148**, 237–250.

508   [29]   Fernandez-Lafuente R., Armisén P., Sabuquillo P., Fernández-Lorente G., Guisán J.M.,

509   Chem. Phys. Lipids, 1998, **93**, 185–197.

510   [30]   Palomo J.M., Ortiz C., Fernández-Lorente G., Fuentes M., Guisán J.M., Fernández-

511   Lafuente R., Enzyme Microb. Technol., 2005, **36,** 447–454.

512   [31]   Fernández-Lorente G., Palomo J.M., Fuentes M., Mateo C., Guisán J.M., Fernández-

513   Lafuente R., Biotechnol. Bioeng., 2003, **82**, 232–237.

514   [32]   Palomo J.M., Peñas M.M., Fernández-Lorente G., Mateo C., Pisabarro A.G., Fernández-

515   Lafuente R., *et al*., Biomacromolecules, 2003, **4**, 204–210.

516   [33]   Manoel E.A., dos Santos C.S., Freire D.M.G., Fernandez-Lafuente R., Enzyme Microb.

517   Technol., 2015, **71**, 53-57.

518   [34]   Cabrera Z., Fernandez-Lorente G., Fernandez-Lafuente R., Palomo J.M., Guisan J.M., J.

519   Mol. Catal. B Enzym., 2009, **57,** 171–176.

520   [35]   Fernandez-Lorente G., Cabrera Z., Godoy C., Fernandez-Lafuente R., Palomo J.M.,

521   Guisan J.M., Process Biochem., 2008, **43**, 1061–1067.

522   [36]   Rodrigues R.C., Garcia-Galan C., Barbosa O., Hernandez K,, dos Santos J.C.S.,

523   Berenguer-Murcia A., Fernandez-Lafuente R., Curr. Org. Chem., 2015, **19**, 1707-1718.

524   [37]   Taqieddin E., Amiji M., Biomaterials, 2004, **25**, 1937–1945.

525   [38]   Ho K.M., Mao X., Gu L., Li P., Langmuir, 2008, **24**, 11036–11042.

526   [39]   Gu Q., Lin Q., Hu C., Yang B., J. Appl. Polym. Sci., 2005, **95**, 404–412.

527   [40]   Besteti M.D., Freire D.M.G., Pinto J.C., Macromol. React. Eng., 2011, **5**, 518–532.

528   [41]   Cunha A.G., Besteti M.D., Manoel E.A., Da Silva A.A.T., Almeida R. V., Simas A,B,C,

529   *et al*., J. Mol. Catal. B Enzym., 2014, **100**, 59–67.

530   [42]   Rodrigues R.C., Fernandez-Lafuente R., J. Mol. Catal. B Enzym., 2010, **64**, 1–22.

531   [43]   Fernandez-Lafuente R., J. Mol. Catal. B Enzym., 2010, **62**, 197–212.

532   [44]   Anderson E.M., Larsson K.M., Kirk O., Biocatal. Biotransformation, 1998, **16**, 181–204.

533   [45]   Uppenberg J., Hansen M.T., Patkar S., Jones T.A., Structure, 1994, **2**, 293–308.

534   [46]   Derewenda Z.S., Derewenda U., Dodson GG., J. Mol. Biol., 1992, **227**, 818–839.

535   [47]   Derewenda U., Swenson L., Green R., Wei Y., Yamaguchi S., Joerger R. *et al*., Protein

536   Eng., 1994, **7**, 551–7.

537   [48]   Clausen K., Eur. J. Lipid Sci. Technol., 2001, **103**, 333–340.

538   [49]   De Maria L., Vind J., Oxenbøll K.M., Svendsen A., Patkar S., Appl. Microbiol.

539   Biotechnol., 2007, **74**, 290–300.

540   [50]   Bastida A., Sabuquillo P., Armisen P., Fernández-Lafuente R., Huguet J., Guisán J.M.,

541   Biotechnol. Bioeng., 1998, **58**, 486–493.

542   [51]   Dos Santos J.C.S., Rueda N., Torres R., Barbosa O., Gonçalves, L.R.B. Fernandez-

543   Lafuente R., Proc. Biochem., 2015, **50**, 918-927.

544   [52]   Dos Santos J.C.S., Rueda N., Sanchez A., Villalonga R., Gonçalves L.R.B., Fernandez-

545   Lafuente R., RSC Advances, 2015, **5**, 35801-35810.

546   [53]   Jaeger K.-E., Ransac S., Koch H.B., Ferrato F., Dijkstra B.W., FEBS Letters, 1993, **332**,

547   143-149.

548   [54]   Cygler M., Schrag J.D., BBA - Mol. Cell Biol. L., 1999, **1441**, 205-214.

549   [55]   Palomo J.M., Fuentes M., Fernández-Lorente G., Mateo C., Guisan J.M., Fernández-

550   Lafuente R., Biomacromol., 2003, **4**, 1-6.

551   [56]   Fernández-Lorente G., Palomo J.M., Fuentes M., Mateo C., Guisán J.M., Fernández-

552   Lafuente R., Biotechnol. Bioeng., 2003, **82**, 232-237.

553   [57]   Wilson L., Palomo J.M., Fernández-Lorente G., Illanes A., Guisán J.M., Fernández-

554   Lafuente R., Enzyme Microbial Technol., 2006, **39**, 259-264.

555   [58]   Palomo J.M., Ortiz C., Fernández-Lorente G., Fuentes M., Guisán J.M., Fernández-

556   Lafuente R., Enzyme and Microbial Technol., 2005, **36**, 447-454.

557   [59]   Palomo J.M., Ortiz C., Fuentes M., Fernandez-Lorente G., Guisan J.M., Fernandez-

558   Lafuente R., J. Chromatogr. A, 2004, **1038**, 267-273.

559   [60]   Pinto M.C.C., Freire D.M.G., Pinto J.C., Molecules, 2014, **19,** 12509-12530.

560   [61]   Besteti M.D., Cunha A.G., Freire D.M.G., Pinto J.C., Macromol. Mater. Eng., 2014, **299**,

561   135-143.

562   [62]   Lenzi M.K., Silva F.M., Lima E.L., Pinto J.C., J. Appl. Polym. Sci., 2003, **89**, 3021-

563   3038.

564   [63]   Lombardo D., Guy O., Biochim. Biophys. Acta, 1981, **657**, 425–437.

565   [64]   Bradford M.M., Anal. Biochem., 1976, **72**, 248-254.

566   [65]   Hernandez K., Garcia-Verdugo E., Porcar R., Fernandez-Lafuente R., Enzyme Microb.

567   Technol., 2011, **48**, 510-517.

568   [66]   Dos Santos J.C.S., Rueda, N. Sanchez, A., Villalonga R., Gonçalves, L.R.B., Fernandez-

569   Lafuente R., RSC Advances, 2015, **5**, 35801-35810.

570   [67]   Rueda N., Dos Santos J.C.S., Torres R., Ortiz C., Barbosa O., Fernandez-Lafuente R.,

571   RSC Advances, 2015, **5**, 11212-11222.

572 [68] Rodrigues R.C., Ortiz, C., Berenguer-Murcia A., Torres R., Fernández-Lafuente R.

573 Chem. Soc.Rev. 2013, **42,** 6290-6307.

574

575

576 **FIGURE LEGENDS**

577

578 **Figure 1.** Scheme of the production of core-shell particles by simultaneous suspension and

579 emulsion polymerization process.

580 **Figure 2**. Influence of the co-monomer feed flow rate on average particle diameter.

581 **Figure 3**. Effect of the comonomer feed flow rate on the morphological properties of the

582 particles: (A) Specific area; (B) Volume of pores; (C) Average pore diameter.

583 **Figure 4.** Optical micrographs of the produced polymeric supports (the length of the ruler is

584 equivalent to 100 μm): (A) compact PS-co-DVB particles; (B) core-shell PS/PS

585 particles; (C) core-shell PS-co-DVB/PS-co-DVB particles.

586 **Figure 5.** Scanning electron micrographs of the polymeric particles: (A) PS-co-DVB core

587 particles; (B) core-shell PS/PS particles; (C) core-shell PS-co-DVB/PS-co-DVB

588 particles.

589 **Figure 6.** Immobilization courses of different enzymes (10 U) onto different supports: (A)

590 CALB; (B) RML; (C) TLL; (D) LU.

591 PS-co-DVB/PS-co-DVB supports are represented by squares; PS/PS supports are

592 represented by triangles; octyl-agarose supports are represented by circles.

593 Dotted lines represent the suspension activities; continuous lines show the

594 supernatant activities.

595 **Figure 7.** **Re-use of different enzyme biocatalysts** on hydrolysis of triacetin: (A) CALB; (B)

596 RML ; (C) TLL; (D) Lecitase. Rhombi: commercial preparations; PS-co-DVB/PS-

597 co-DVB: triangles; PS/PS: squares.

598

599   Figure 1
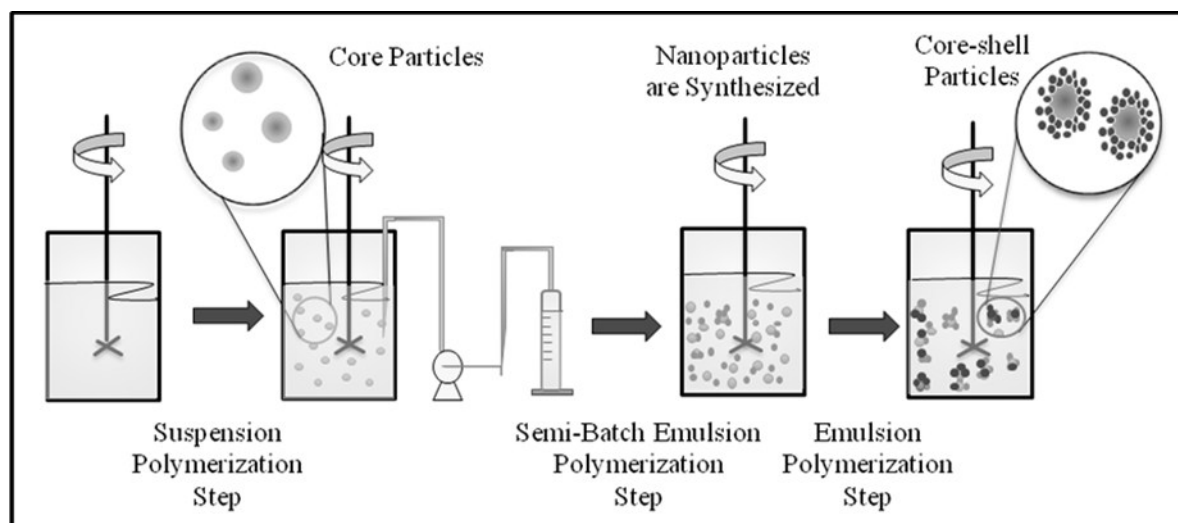
600

601 Figure 2
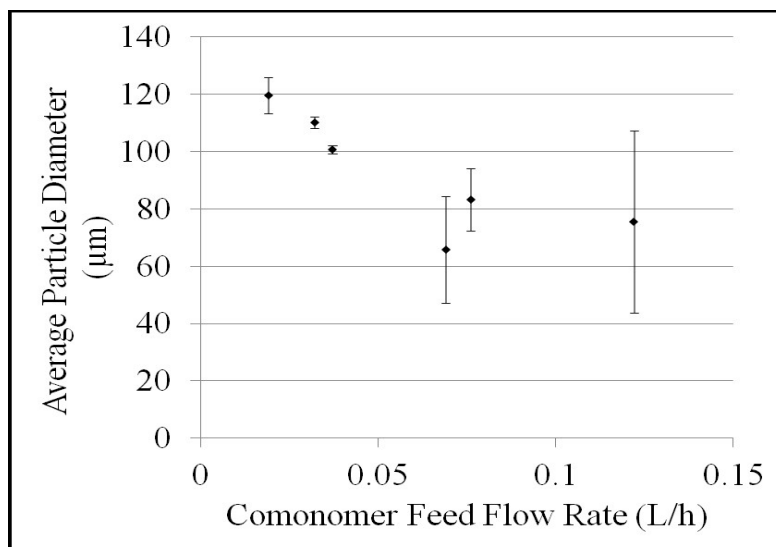
602

603

604

605

606

607

608

609

610

611

612

613

614

615

616

617

618

619

620   Figure 3

621

622   (A)   (B)

623

624   (C)
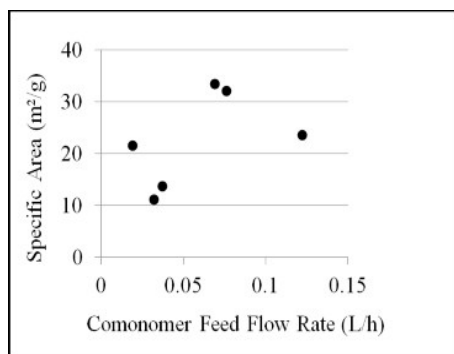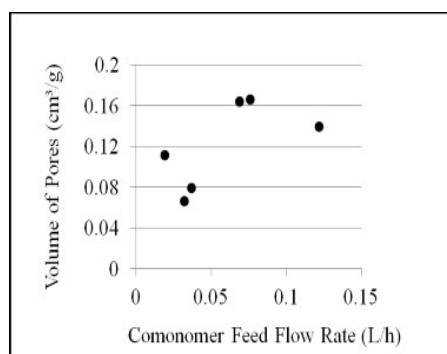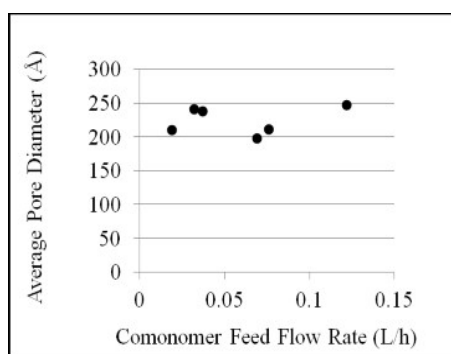
625

626

627

628

629

630

631

632

633

634

635

636

637

Figure 4

638

639 (A) (B)

640

641 (C)
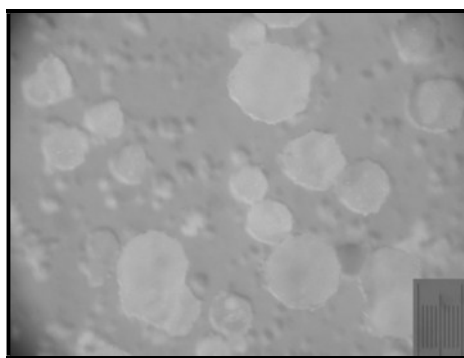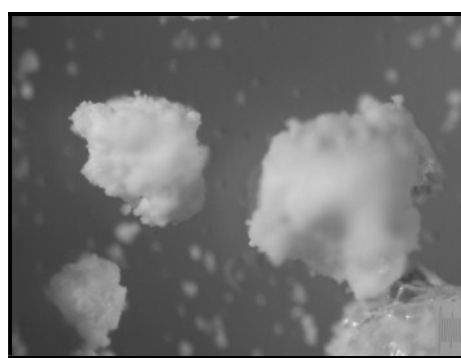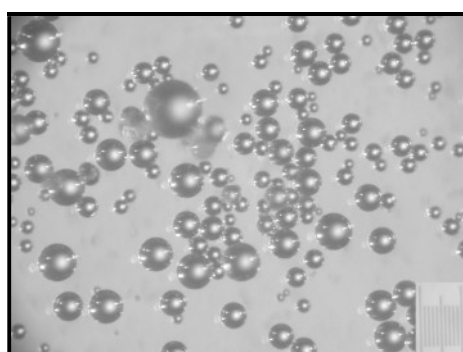
642

643

644

645

646

647

648

649

650

651

652

653

654   Figure 5
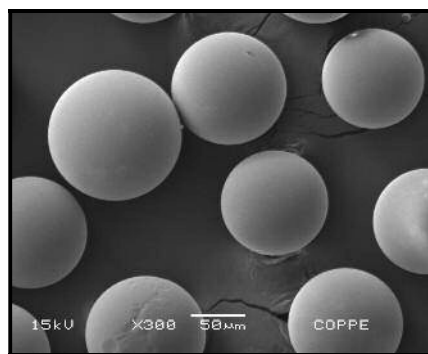
655
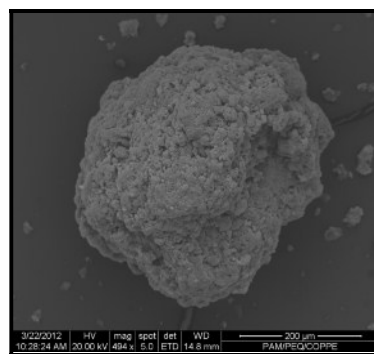
656   (A)   (B)
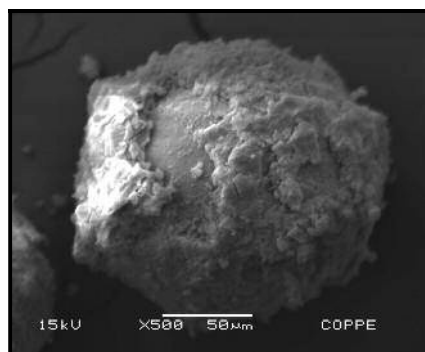
657

658   (C)

659

660

661

662

663

664

665

666

667

668

669

670

671   Figure 6

672

673   (A)   (B)

674

675   (C)   (D)
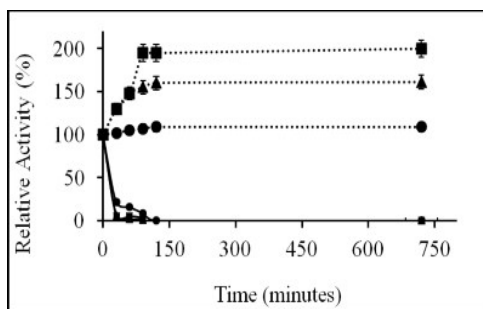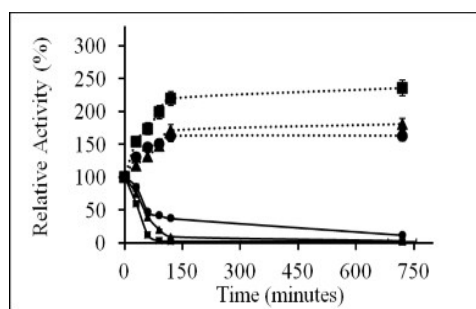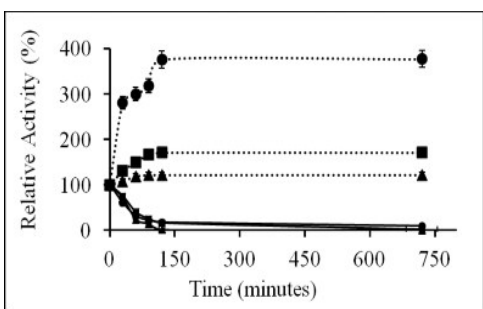
676

677

678

679

680

681

682

683

684

685

686

687

688

689

32

690   Figure 7

691

692   (A)   (B)

693

694   (C)   (D)

695

696

697

698

699

700

701

702

703

704

705

706

707

708
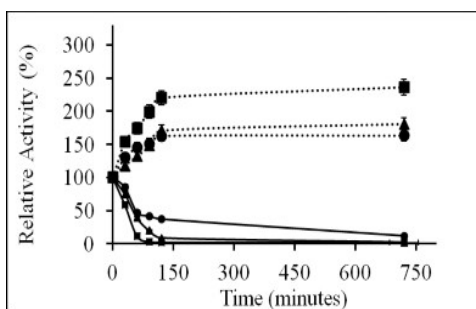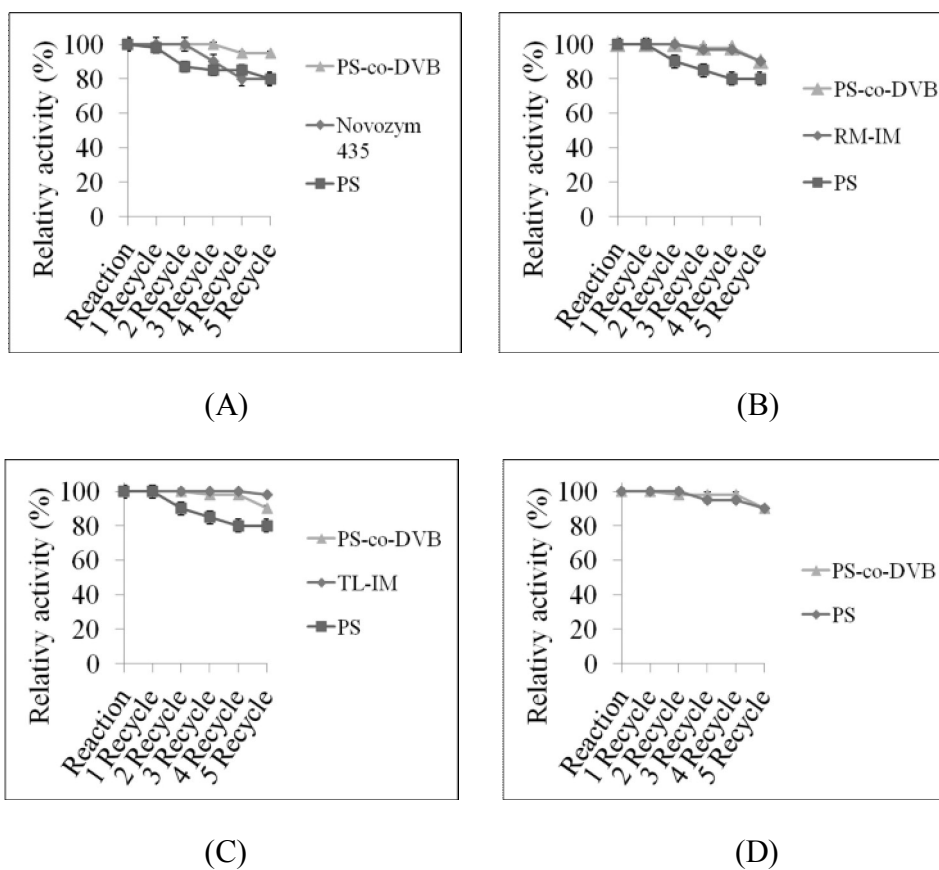
709 **Table 1.** Operational condition employed for each polymerization reaction.

	Operational Condition	
Reaction	Ratio of (S:DVB)	Comonomer Feed Flow Rate (L/h)
1	3:1	-
2	3:1	0.032
3	3:1	0.076
4	3:1	0.122
5	3:1	0.019
6	3:1	0.037
7	3:1	0.069

34

710   **Table 2.** Average diameters of the produced particles.

Supports	Average particle diameter (d_{50}) (µm)
PS/PS[a]	114.6±1.3
PS-co-DVB/PS-co-DVB[a]	65.8±18.6
PS-co-DVB[b]	92.2±1.1

711   [a] Core-shell supports; [b] The compact cores particles alone.
712
713
714
715
716
717
718
719
720
721
722
723
724
725
726
727
728
729
730
731

732 **Table 3.** Morphological characteristics of the produced supports used on enzyme

733 immobilization.

Supports	Specific area (m^2/g)	Average pore diameter (Å)	Specific volume of pores (m³/g)
PS/PS[a,b]	27.3	287.6	0.20
PS-co-DVB/PS-co-DVB[b]	33.4	197.2	0.16
PS-co-DVB[c]	0.0025	-	-

734 [a] Pinto *et al*., 2014 [60]; [b] Core-shell support; [c] The compact core particles alone.
735

736

737   **Table 4.** Half-lives (expressed in minutes) of the different biocatalysts under different

738   inactivation conditions. Experiments were performed as described in Section 2.

Lipases	Supports	Inactivation conditions*	
		pH 7, 70 ºC	90% DMF, pH 7, 25 ºC
CALB	PS/PS	10.0±0.5	45±1.0
	PS-co-DVB/PS-co-DVB	30±0.5	25±1.0
	Octyl-Agarose	28±1.5	8±1.0
RML	PS/PS	5.0±0.2	5.0±1.0
	PS-co-DVB/PS-co-DVB	20±0.2	18±0.8
	Octyl-Agarose	10±0.5	13±2.0
TLL	PS/PS	120±1.0	20±1.0
	PS-co-DVB/PS-co-DVB	40±0.1	40±0.5
	Octyl-Agarose	165±5.0	22±3.0
LU	PS/PS	40±0.5	15±1.0
	PS-co-DVB/PS-co-DVB	5±0.2	40±1.0
	Octyl-Agarose	19±4.0	8±1.5

739

740   The number of replicates of these analyses were 6 (n=6) and the experimental errors were
741   calculated with confidence level of 95%.

742 **Table 5.** Activity of different enzyme biocatalysts in the hydrolysis of triacetin. Experimental

743 conditions are described in Section 2.

744

Hydrolysis of triacetin		
	Biocatalyst	**Activity (μmol.(min.g)$^{-1}$)**
CALB	Novozym 435	207±1.2
	PS/PS	214±1.0
	PS-co-DVB/PS-co-DVB[*]	105±0.8
	Octyl-Agarose	89±0.5
	RM-IM	28.1±0.5
RML	PS/PS	47.0±0.3
	PS-co-DVB/PS-co-DVB	50.0±0.6
	Octyl-Agarose	42.8±0.5
	TL-IM	15.1±0.2
TLL	PS/PS	32.1±0.6
	PS-co-DVB/PS-co-DVB	32.2±0.5
	Octyl-Agarose	27.3±1.1
	PS/PS	20.8±1.1
LU	PS-co-DVB/PS-co-DVB	31.3±0.8
	Octyl-Agarose	28.3±0.5

759 Analyses were conducted in triplicate (n=3) and the experimental errors were calculated with
760 confidence level of 95%.

761

762

38

763   **Table 6.** Activity of different enzyme biocatalysts in the hydrolysis of R methyl mandelate and

764   VR/VS ratio. Experimental conditions are described in Section 2.

Hydrolysis of R-Methyl Mandelate			
	Biocatalyst	**Activity (μmol.(min.g)$^{-1}$)**	**VR/VS**
CALB	Novozym 435	140±1.2	1.35
	PS/PS	210±2.2	1.65
	PS-co-DVB/PS-co-DVB	260±1.6	2.65
	Octyl-Agarose	210±2.8	2.30
RML	RM-IM	0.51±0.3	0.32
	PS/PS	0.57±0.6	0.31
	PS-co-DVB/PS-co-DVB	0.82±0.1	0.28
	Octyl-Agarose	0.74±0.1	0.24
TLL	TL-IM	1.0±0.2	2.3
	PS/PS	1.1±0.1	1.64
	PS-co-DVB/PS-co-DVB	2.3±0.1	1.67
	Octyl-Agarose	1.1±0.2	1.57
LU	PS/PS	0.9±0.2	0.81
	PS-co-DVB/PS-co-DVB	2.6±0.2	1.45
	Octyl-Agarose	0.95±0.1	0.95

765   Analyses were conducted in triplicate (n=3) and the experimental errors were calculated with
766   confidence level of 95%.

lipase
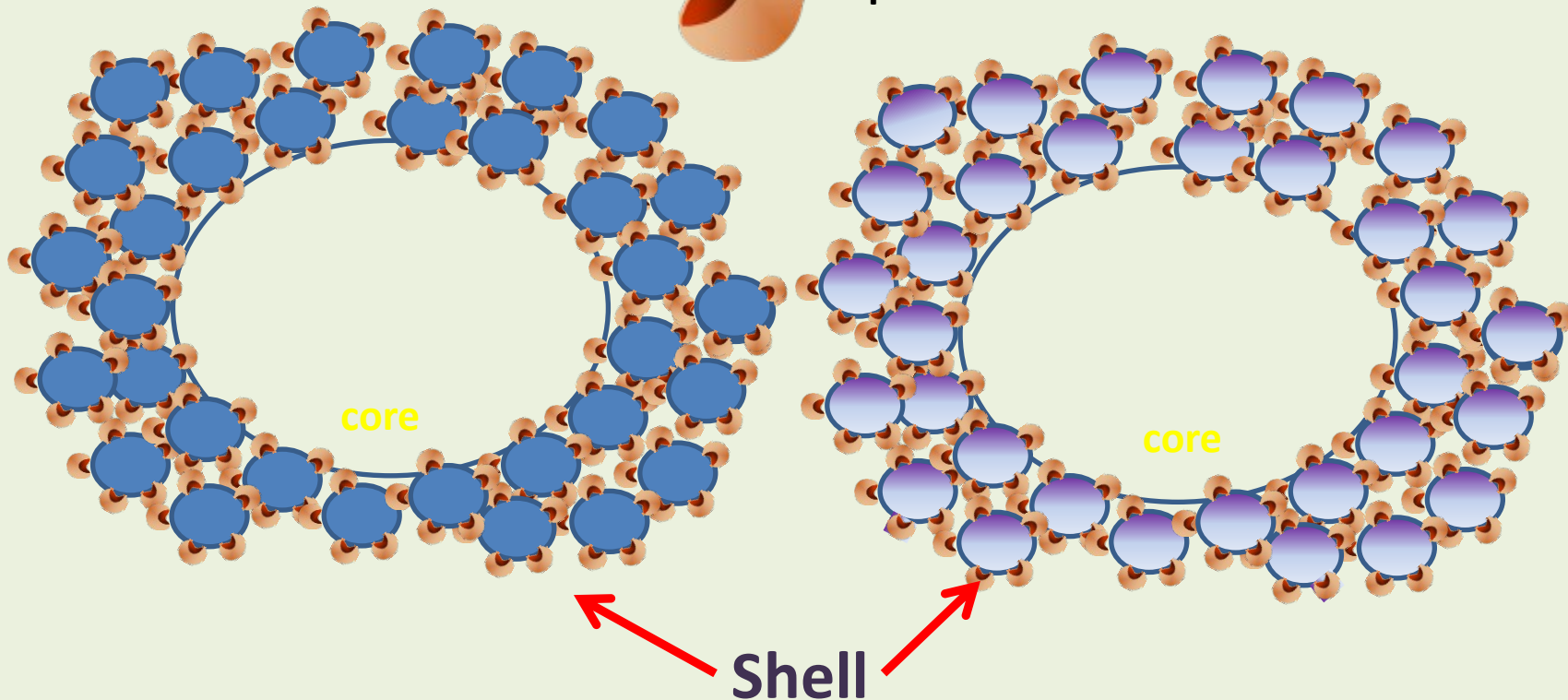
core

core

Shell

DIFFERENT HYDROPHOBIC
CORE-SHELL PREPARATION
(POLYMER, POLYMERIZATION
CONDITIONS)

DIFFERENT CORE-SHELL
SUPPORTS PERMIT
TO TUNE THE PROPERTIES
OF LIPASES

DIFFERENT CORE-SHELL
PROPERTIES